

EEG-Based Emotion Recognition  
Chris Manna  
EE675

**Abstract:**

This study investigates the classification of discrete emotions using EEG signals from the SEED-V dataset, employing both a Support Vector Machine and Multilayer Perceptron trained on both differential entropy and power spectral density. While testing accuracy results of the models were low, the high variability in the per-subject model emphasizes the variability in individual emotional responses suggesting that a dimensional model may be more effective. In addition, the analysis of the brain topography emphasizes that emotions are not evoked from a singular neural region aligning with the Psychological Constructionist Perspective.

**1. Introduction**

Emotions play a pivotal role in shaping human behavior, influencing mental health, interpersonal relationships and the learning process. Despite their significance, the mechanism of these emotions within the brain remain enigmatic, giving rise to divergent perspectives on their generation.

One school of thought, known as the Psychological Constructionist Perspective, theorizes that emotions lack dedicated brain regions and instead emerge from a result of complex interactions between multiple brain regions. Whereas others theorize that certain emotions are evoked from specific parts of the brain.

Building an understanding of the brain is imperative to further understanding emotions. This has led to a growth in interest in Brain-Computer-Interface (BCI) research dedicated to the classification of emotions. The most common approach to this is to use Electroencephalography (EEG) signals.

Brain waves are oscillating signals that have a magnitude of a few millionths of a volt which serve as a fundamental indicator of neural activity. Currently it is believed that there are five distinct brainwave frequencies: Gamma, Beta, Alpha, Theta, and Delta. Each of these frequencies is believed to correspond to a different brain state. For instance, Gamma waves are typically associated with Heightened Awareness.

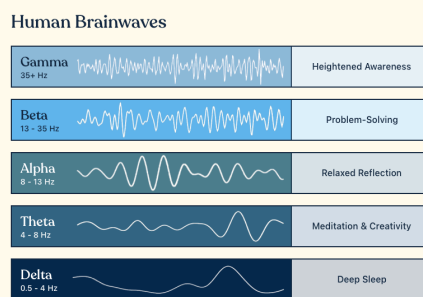


Figure 1: Brainwave Frequencies

The goal of this paper is to accurately classify five discrete emotions based on these EEG waves utilizing the SEED-V dataset. Through a meticulous analysis of various models trained on different subjects and frequencies, we aim to discern the specific brain regions and frequencies associated with the generation of distinct emotions as well as understand the variability in these regions' activations across individuals.

## 2. Emotion Classification Approaches and Dataset Overview

### A. Emotion Classification

There are two ways to classify emotion: discrete and dimensional categorization. Discrete Categorization assigns specific, distinct labels to emotions emphasizing their distinct and distinguishable features. In contrast, dimensional categorization involves understanding emotions within a multidimensional space. For instance, a common approach is to base emotion on the value of arousal and valence as seen below. The SEED-V dataset and consequently my study as well utilizing discrete classification.

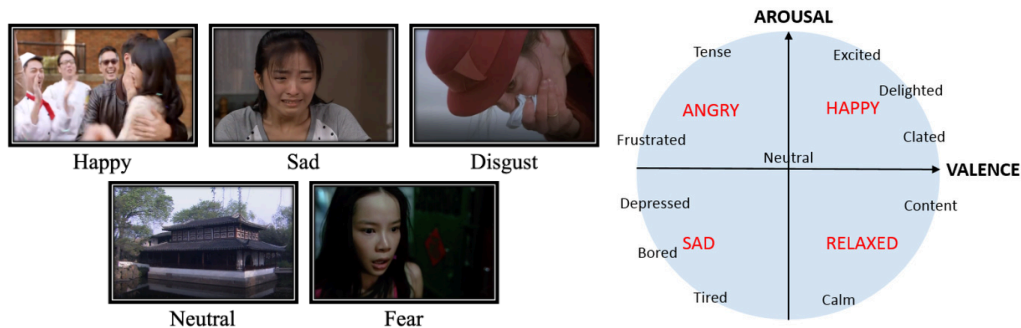


Figure 2: Types of Classification

### B. SEED-V Dataset Overview

The SEED-V dataset, developed by Shanghai Jiao Tong University, serves as the foundational component of this study. The dataset aims to capture the EEG and eye movement signals of five emotions: Happy, Sad, Disgust, Neutral, and Fear. [1]

These emotions would be evoked by having the participants watch short video clips. The video clips were selected from a separate preliminary study using twenty participants. In this study, the participants looked at various clips and rated the level of a certain emotion each they felt the clip evoked on a scale of 1-5. The top-rated clips for each emotion, totaling nine clips per emotion, were then incorporated into the SEED-V dataset, ensuring a unique video clip for each trial in every session.

The experiment involved 16 patients, who participated in three sessions with 15 trials per session resulting in 720 total trials, 144 per emotion. At the start of each trial, the subject would watch a brief abstract about the content and the desired emotion to be elicited before watching the clip. The clips varied in length from 2-4 minutes, followed by a 15-30 second rest period for self-evaluation. During the self-evaluation the subject would rank how well they thought the clip evoked the desired emotion in them.

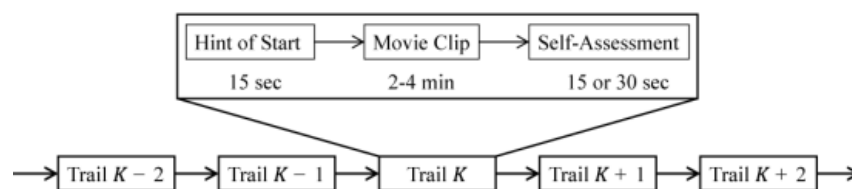


Figure 3: Trial Details

The 62-channel ESI NeuroScan System and SMI ETG eye-tracking glasses were used to record EEG and eye movement signals simultaneously. While the study fuses the eye movement data in combination with the EEG signals, this investigation specifically focuses on the EEG signals. By training and testing models solely on EEG data, I aim to draw meaningful insights into the role of EEG signals in emotion classification. The SEED-V study involves training and testing the models on solely EEG signals, solely eye tracking movements and a fusion of both features.. I will be comparing my results exclusively to their EEG only models.

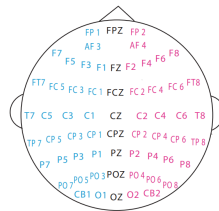


Figure 4: EEG Cap Layout for 62 Channels

### 3. Methods

#### A. Preprocessing

Measured EEG signals inherently contain a large amount of noise and artifacts. Artifacts are signals recorded by the EEG but not produced by the brain. For instance, whenever you blink a spike occurs in the recorded EEG data. Removing these is essential to the success of the model. Initially a bandpass filter from 1 to 50 Hz is applied to all the EEG signals. Having a low cutoff frequency of 1 Hz removes any DC drift that occurs within the signal. In addition, EEG waves occur at frequencies between 1 to 50 Hz, thus removing any frequencies higher than that will also cut off undesired noise. Afterwards, Eye movement artifacts were then removed from the EEG signal using Independent Component Analysis (ICA). Specifically 20 independent components were generated, any component related to Vertical EOG, Horizontal EOG, and FPZ channels were extracted and excluded from the signal. In addition, the ground, EOG, and FPZ channels were then removed leaving us with 61 channels for our data.

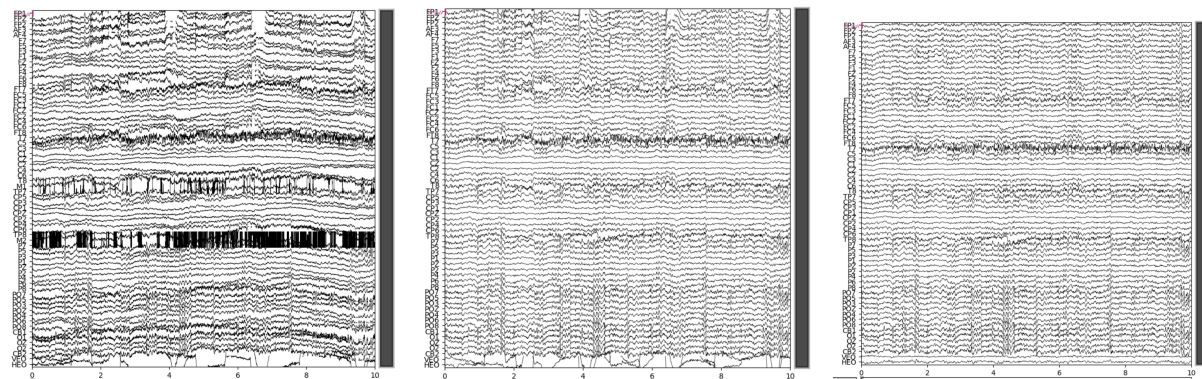


Figure 5: Original EEG signal, Filtered EEG Signal, Artifact Removed EEG Signal

Post-artifact removal, the signal was downsampled to 200 Hz to alleviate the computational burden. The Power Spectral Density (PSD) of each Frequency Band was computed using the Short Time Fourier Transform. This involved a 4-second Hanning window with no overlap

providing insights into how the frequency magnitudes change with time. With 61 channels and 5 frequency bands, this computation resulted in a 305 dimension for each time slot within every trial.

To do this I performed the Short Time Fourier Transform over the signal utilizing a 4 second hanning window with no overlap. This gives the changes in the magnitude of the frequency over time. I then isolated the frequency components within each band and took the average value across the frequencies. This was done for all 62 channels resulting in 305 dimensions for each row. Where each row represents the average frequency within the band over that 4 second period. Thus there will be a total\_time\_of\_clip/4 number of data points for each trial.

For feature selection, two common indexes related to frequency used in related studies are Power Spectral Density as well as Differential Entropy. Many of these papers have stated that Differential Entropy has given better results than the Power Spectral Density. This study will include a comparison of the accuracy of both of these indices.

One can calculate Differential Entropy of a signal, which quantifies the amount of uncertainty, from the following integral.

$$h(x) = E[-\log(f(x))] = - \int_{-\infty}^{\infty} f(x) \log(x) dx$$

If X follows a gaussian distribution, Differential Entropy can then be defined as

$$h(x) = - \int_{-\infty}^{\infty} \frac{1}{\sqrt{2\pi\sigma^2}} e^{-\frac{(x-\mu)^2}{2\sigma^2}} \log\left(\frac{1}{\sqrt{2\pi\sigma^2}} e^{-\frac{(x-\mu)^2}{2\sigma^2}}\right) dx = \frac{1}{2} \log(2\pi e \sigma^2)$$

While the EEG signal itself is not normally distributed, in previous studies it has been found that the EEG signal when filtered to a specific frequency band becomes normally distributed [2]. This was verified by taking random points from a time signal within a frequency band and comparing it to a normal distribution. The Q-Q plot of this can be seen below. The distribution closely follows the normal distribution with only a few outliers on the tail end most likely due to noise and artifacts not being completely removed.

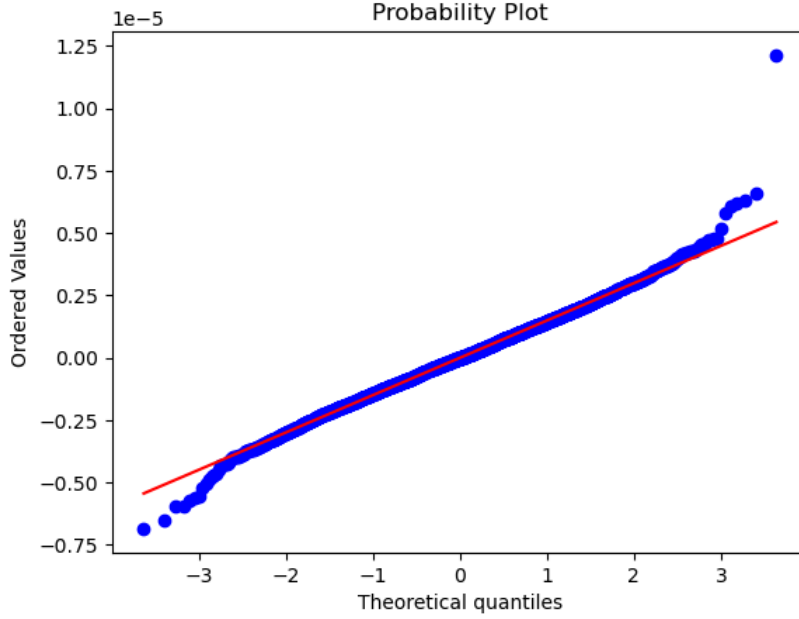


Figure 6: Frequency Band Time Signal against Normal Distribution Q-Q Plot

Therefore for a fixed frequency band ,  $i$  The differential entropy becomes defined as:

$$h(x) = \frac{1}{2} \log(2\pi e \sigma_i^2)$$

This signal variance can then be estimated as:

$$\hat{\sigma}^2 = \frac{1}{N} \sum_{i=0}^{N-1} x_i^2$$

Notice how the signal variance of  $X$  is simply the average energy. Consequently this can then be related to the Energy Spectrum,  $P_i$ :

$$\sum_{i=0}^{N-1} |x_i|^2 = \frac{1}{N} \sum_{k=0}^{N-1} |X_k|^2 = P_i$$

The energy spectrum is equivalent to the signal variance multiplied by the constant coefficient  $N$ , which is the length of the fixed time window (4 seconds \* sample frequency). Thus the differential entropy can be calculated as:

$$h(x) = \frac{1}{2} \log(P_i) + \frac{1}{2} \log\left(\frac{2\pi e}{N}\right)$$

After Power Spectral Density and Differential Entropy features were calculated. A linear dynamic system (LDS) was then used to smooth out the features over time. This Linear dynamic system was modeled and implemented as follows [3] [4].

- Let  $\eta$  be the emotional state, this can then be mapped to the emotional-state related EEG signal  $\eta \rightarrow E_\eta$
- The EEG signal is further mapped to an EEG index,  $F_i: E_\eta \rightarrow X_i$ , where  $X_i$  signifies EEG index

Even after filtering, and artifact removal there is still difference between our measured EEG feature  $F_i(E_{\eta t} + E_{Ot})$  and true EEG feature  $F_i(E_{\eta t})$ , where  $E_{Ot}$  represents the Emotion-unrelated EEG. This discrepancy can be modeled as gaussian noise,  $\omega_t$ , as seen below:

$$F_i(E_{\eta t} + E_{Ot}) = F_i(E_{\eta t}) + \omega_t$$

In addition, Emotional states are time dependent. This temporal change can be considered gaussian, where  $A$  represents the transition matrix and  $v_t$  represents gaussian noise.

$$F_i(E_{\eta t}) = A F_i(E_{\eta t-1}) + v_t$$

This gives rise to the following LDS system:

$$\begin{aligned} x_t &= z_t + \omega_t, \\ z_t &= A z_{t-1} + v_t, \end{aligned}$$

The parameters  $\{A, Q, R, \bar{\omega}, \bar{v}, \pi_0, S_0\}$  can be determined through the observation matrix sequence  $\{x_t\}$  using the maximum likelihood through the EM algorithm.  $A$  represents the state transition matrix,  $Q$  represents the variance of  $\omega_t$ ,  $R$  is the variance of  $v_t$ , and  $\pi_0, S_0$  is distribution of the initial latent state. After estimating the parameters, Kalman smoothing is then used to better fit the observed data.

## B. Model Selection and Training

The two models, support vector machine (SVM) and Multilayer Perceptron (MLP), were used to classify the data. To reduce the data. Principal Component Analysis (PCA) was performed on the data set, reducing the data while retaining 95% of its original covariance.

To prevent data leakage, Session 3 was exclusively used for testing, whereas Session 1 and 2 were utilized for training, resulting in an approximate 66.66%-33.33% train-test split. Both the SVM and MLP undergo hyperparameter tuning via cross validation.

Again to ensure no leakage between the folds when training, the training data was split by trials, ensuring a specific trial did not get split into multiple folds. This approach aimed at maximizing the model's generalization to new data.

A generalized model for all subjects was trained using both SVM and MLP using both Power Spectral Density and Differential Entropy. The best-performing model and dataset combination was then used to train additional models. Notably, the original paper trained a model for each subject. Consequently a model was created for each subject. In addition, a model was created for each frequency band. Additionally, models were created for each frequency band, using data from all subjects for training.

## 4. Results & Discussion

### A. Generalized Model

All combinations of MLP, SVM, Differential Entropy and Power Spectral yielded similar accuracies, with only slight differences. For Differential entropy the testing accuracies were 30.29% for MLP and 29.43% for SVM. For Power Spectral Density the testing accuracies were 32.57% for MLP and 29.47% for SVM. The confusion matrices for these tests can be seen below.

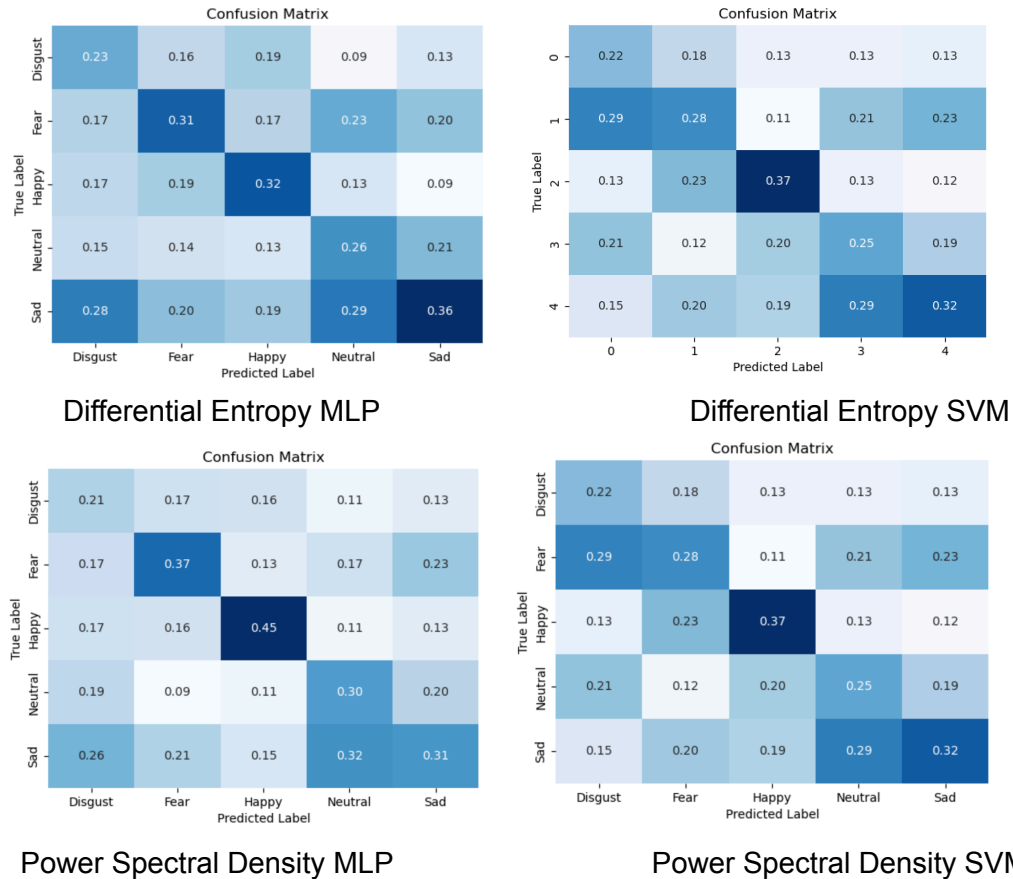


Figure 7: Confusion Matrix for Generalized Models

While the accuracy for Power Spectral Density was slightly higher, the overall low accuracy suggests challenges in classification. The models are only marginally better than chance (20%), indicating potential issues during preprocessing.

### B. Per Subject Model

The MLP model with Power spectral Density was used for the individual subject models. In comparison to the general model, the accuracy does slightly improve when training on a single subject. While the mean accuracy across all the models was 35.9%, certain per-subject models achieved higher accuracies, with some reaching as much as 56.8%, – a substantial enhancement compared to the generalized model. The standard deviation for the per person model accuracy was extremely high, Some individuals models had accuracies as low as 22.1%

which means the model is essentially no better than chance. This high variability in model accuracy emphasizes the diverse nature of individuals' emotional responses.

Model Accuracy Per Subject		
Subject	Accuracy	Statistics
1	47.6%	$\bar{X} = 35.9\%$
2	56.8%	$\sigma = 11.1\%$
3	49.8%	
4	31.5%	
5	25.2%	
6	31.8%	
7	31.1%	
8	41.3%	
9	55.2%	
10	26.9%	
11	25.3%	
12	26.1%	
13	42.7%	
14	22.1%	
15	26.1%	
16	35.6%	

Table 1

In the original SEED-V study the average testing accuracies for their per model subject was  $69.50 \pm 10.28$ . Although their accuracy surpassed that of this study, the variance was similarly high, indicating substantial variability in emotions from subject to subject. Notably, the subjects with the highest accuracy in my study aligned with those in the original paper, highlighting the need for enhanced pre-processing and training to improve overall accuracy.

### C. Per Frequency Band Model

When evaluating the one frequency band models, unsurprisingly, the testing accuracy decreased suggesting that emotions are a complex activation of multiple EEG frequency bands. The Higher frequency bands Beta and Gamma had a higher accuracy potentially indicating these waves may play a more active role in the generation of emotions.



Model Accuracy Per Frequency Band					
Frequency Band	Delta	Theta	Alpha	Beta	Gamma
Testing Accuracy	21.09%	21.25%	22.9%	25.9%	26.8%
				$\bar{X} = 23.6\%$	$\sigma = 2.4\%$

Table 2

D. Neural Patterns of Evoked Emotions

The topography of the average power spectral density across each frequency band was plotted. Yellow represents a higher power spectral density whereas a darker color represents a lower.

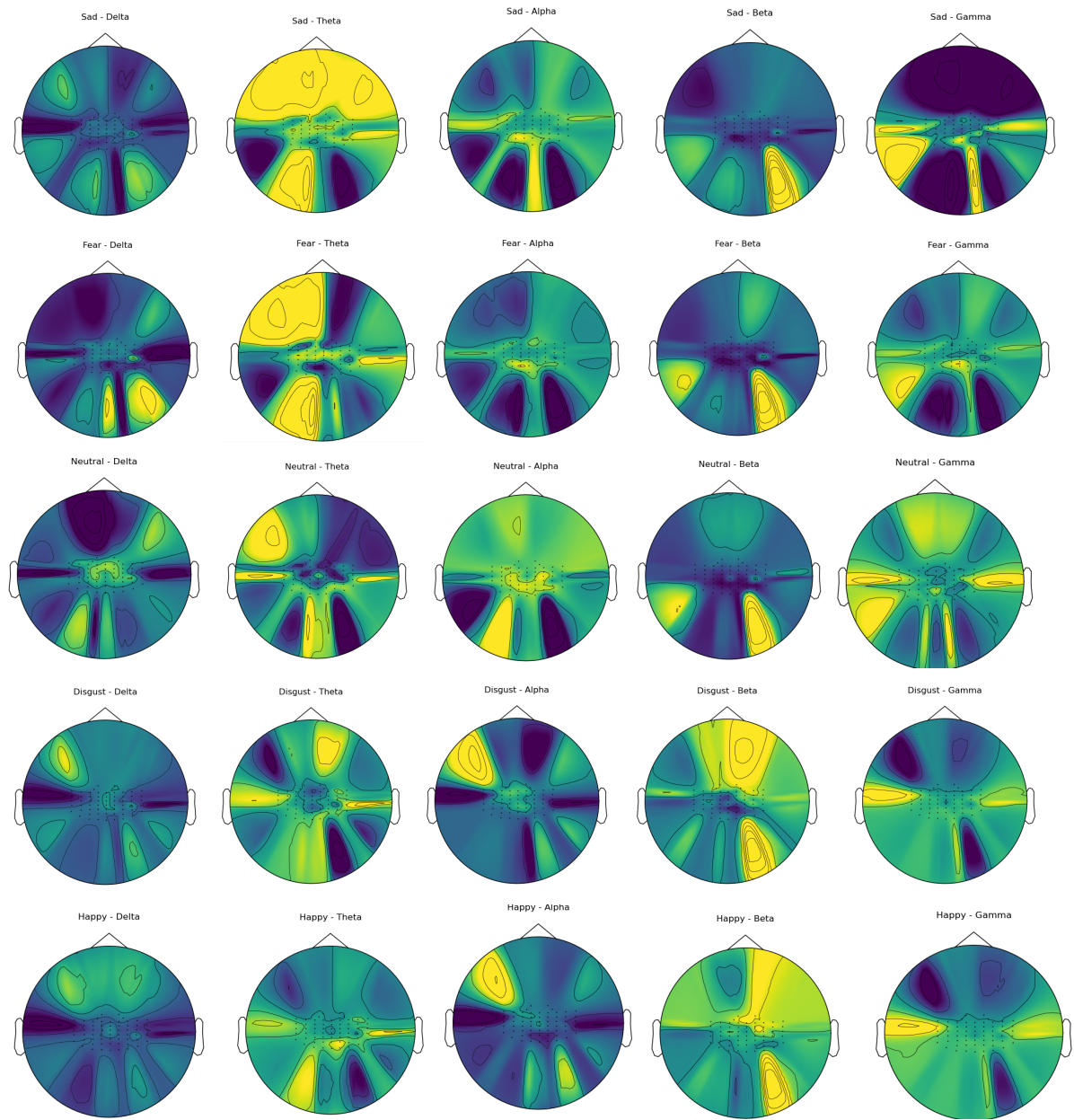


Figure 8: Topography of Each Frequency Band for each Emotion

Surprisingly, Theta waves, generally associated with meditation and creativity, exhibit a substantial spectral density when the subject experiences sadness and fear. Particularly, sadness shows a significant spectral density in the front half of the brain. This observation suggests a peculiar similarity between the numbingness of sadness and the meditative state or challenges the basic associations of these waves mentioned at the beginning of the paper. On the other hand, Gamma waves, linked to heightened awareness, display relatively high activation in all emotions except sadness. This aligns with the notion that individuals experiencing sadness tend to be less aware of their surroundings.

Overall, each emotion demonstrates a high power spectral densities across various frequencies and numerous areas of the brain. This challenges the notion that certain emotions correspond to distinct parts of the brain. Consequently this topography map supports the Psychological Constructionist Perspective exemplifying emotions are a complex process evoking various parts of the brain.

## **5. Conclusion**

In conclusion, emotions evoked in the brain are a remarkably intricate process that involves activation of various regions throughout the neural landscape. This is emphasized by challenges I experienced during my project particularly my low testing accuracy. My low testing accuracy can most likely be attributed to implementation of the linear dynamic system as well as hyper parameter tuning. The extensive computational demands, especially in smoothing the large dataset, led to time constraints that affected the fine-tuning of iterations and applications.

Despite these challenges, Power Spectral Density ended up having a slightly higher accuracy than Differential Entropy. This suggests the potential to possibly look at utilizing this feature in future studies. Further exploration and utilizing of this feature may provide additional insights on emotional dynamics within the brain

The notable variance observed in the subject-to-subject models underscores the inherent challenges in evaluating emotions. Evaluating an emotion is an extremely vague and subjective concept. How well did each clip evoke that emotion for each subject? While the participants provided their evaluations, neither the original study nor mine employed specific techniques to account for the inherent subjectivity in emotional responses. Addressing this challenge could enhance the robustness and reliability of future studies aiming to decode emotions based on EEG signals. This variance could also suggest that neural patterns are distinct per person and a model cannot be generalized.

This substantial variance in the per-subject models, in combination with examining the topography of frequency bands for each emotion, suggests a dimensional model may be more effective than a discrete one. One can experience both happiness and fear at the same time as well as different levels of happiness. This perspective aligns with datasets like DEAP, which aim to capture the multidimensional nature of emotional experiences. (Funny enough I applied for this dataset and never heard back till about a week ago!) This project served as a valuable learning experience in brain modeling. I hope to improve upon my model further as well as adapt a model from this dataset to use in the DIY EEG reader I made.

## References

- [1] T.-H. Li, W. Liu, W.-L. Zheng, and B.-L. Lu, "Classification of Five Emotions from EEG and Eye Movement Signals: Discrimination Ability and Stability over Time," in *2019 9th International IEEE/EMBS Conference on Neural Engineering (NER)*, San Francisco, CA, USA: IEEE, Mar. 2019, pp. 607–610. doi: 10.1109/NER.2019.8716943.
- [2] Li-Chen Shi, Ying-Ying Jiao, and Bao-Liang Lu, "Differential entropy feature for EEG-based vigilance estimation," in *2013 35th Annual International Conference of the IEEE Engineering in Medicine and Biology Society (EMBC)*, Osaka: IEEE, Jul. 2013, pp. 6627–6630. doi: 10.1109/EMBC.2013.6611075.
- [3] Li-Chen Shi and Bao-Liang Lu, "Off-line and on-line vigilance estimation based on linear dynamical system and manifold learning," in *2010 Annual International Conference of the IEEE Engineering in Medicine and Biology*, Buenos Aires: IEEE, Aug. 2010, pp. 6587–6590. doi: 10.1109/IEMBS.2010.5627125.
- [4] W.-L. Zheng, J.-Y. Zhu, and B.-L. Lu, "Identifying Stable Patterns over Time for Emotion Recognition from EEG." arXiv, Jan. 10, 2016. Accessed: Dec. 07, 2023. [Online]. Available: <http://arxiv.org/abs/1601.02197>